Chalcogenide Letters Vol. 7, No. 3, March 2010, p. 187 - 196

THERMAL STABILITY OF SOME GLASSY COMPOSITIONS OF THE Ge-As-Te TERNARY

L. ALDON, MATHURIN LEH DELI[a*], P.E. LIPPENS, J. OLIVIER-FOURCADE, J.C. JUMAS
Laboratoire des Agrégats, Interfaces et Matériaux pour l'Energie, Institut Charles Gerhardt, UMR 5253 CNRS, Université Montpellier II, Place Eugène Bataillon, F-34095 Montpellier Cedex 5, France
[a] *Laboratoire de chimie des matériaux inorganiques, Université de Cocody, 22 Bp 582 Abidjan 22, Côte D'Ivoire*

Tellerium-based chalcogenide glasses have been studied extensively in the recent past not only because of their technological applications, but also due to their interesting physical properties. Tellerium is a good element for far infrared transmission but is a poor glass former. Glass forming domains are very narrow in binary Ge-Te or As-Te system. Better glass forming ability and thermal stability are observed in presence of arsenic and germanium atoms. These glasses possess a wide optical window that is maximal for the $Ge_{10}As_{20}Te_{70}$ glass (20μm). It made it possible to show that the substitution of germanium by selenium and antimony reduces the physical properties (ρ, Eg, Tg, Tc_1, Tc_2, Tc_1-Tg et T_m). Indeed germanium supports the formation of glasses, contrary to metal antimony.

(Received February 22, 2010; accepted March 1, 2010)

Keywords: Chalcogenide glasses, X-ray diffraction, Thermal behavior, Optical properties

1. Introduction

Vitreous materials have thermo-physical and mechanical properties that make them suitable for many applications in various devices using ligtht wave emission, transmission or detection. These device functions depend on optical and electronic characteristics, such as electrical conductivity[1,2] , the gap width and its nature. Chalcogenide glasses offer a range of infrared transmitting materials that are transparent in the regions of 3-5 μm and 8-14 μm. Thus, observed transmitting ranges in glasses are 0.6-15μm for sulfides, 1-18 μm for selenides and 2-20μm for tellurides. Chalcogenide glasses have also a high refractive index, low optical losses and their possible applications as infrared optical materials have been discussed[3,4]. Glasses of binaries As-Te[5] and Ge-Te[6] have been extensively studied as regards to their optical properties because they are transparent to infrared radiation from 2 to 18μm[7,8]. These glasses are good candidates for exoplanet atmosphere detection[9]. Other studies have been carried out on their electrical properties, density, heat capacities, and electrical properties[10,11].

The Ge-As-Te ternary system shows the existence of the quasi-binary $nGeTe\text{-}As_2Te_3$ crystalline phases (with n = 1, 3, 5) [12,13] separating two glass forming regions [14,15]. We have represented in Fig. 1 the main crystalline phases, and some glassy compositions under investigation in the 'Te-rich' and 'As-rich' regions. Having in mind the fact that the area of glassy state of the Ge-Te and As-Te binary systems is relatively small, and that Te-containing glasses exhibit an increased tendency towards crystallization [16], melt cooling was carried out by quenching in iced water. So, structural information on telluride glasses is needed in order to characterize the local order in these materials. Among the different experimental tools, differential scanning calorimetry and optical absorption spectroscopy provide valuable information for chalcogenide glasses. Structural information from EXAFS[17], ^{125}Te Mössbauer spectroscopy [18], and also electronic properties have been earlier investigated[19,20].

*Corresponding author: lehdeli@netcourrier.com

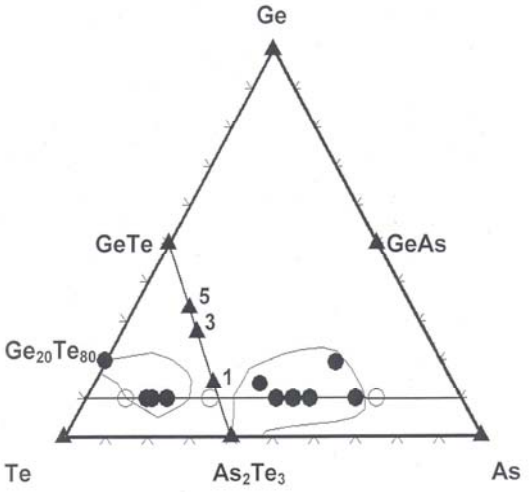

Fig. 1. Glass forming regions in the ternary Ge-As-Te: (▲) crystalline phases. For pseudo-binary As_2Te_3-nGeTe, n values are represented (n = 1, 3 and 5). Chemical compositions of prepared glasses (●) and partially crystallized samples (○) are represented

In the present paper, particular attention is focused on the compositions $Ge_{10}As_{90-x}Te_x$ (with 35<x<80) and their preparation. We are interested in the substitution of As for Te in the widest tie line at 10% germanium.

2. Experimental procedure

Glassy $Ge_{10}As_{90-x}Te_x$ ingots (with 35<x<80) where prepared by melt-quenching method. Chemical mixtures of Ge, As and Te (4N purity) were vacuum sealed (10^{-5}torr) in silica ampoules (3mm id, 4mm od) and slowly heated in a furnace at 1000°C for 8 hours. The contents of the ampoule were about 1g. The ampoules were agitated continuously during the heating process and during several hours at the melting temperature in order to ensure good homogeneity of the glasses. The experimental set-up is shown in Fig. 2. The melt was quenched in iced water at 273K to reach the glassy state of the samples. The quenching rate was estimated to be about 100K/s. Ingots thus obtained were annealed at about 50°C below the glass transition temperature for 8 hours. The same experimental process was used for compositions of the ternary system.

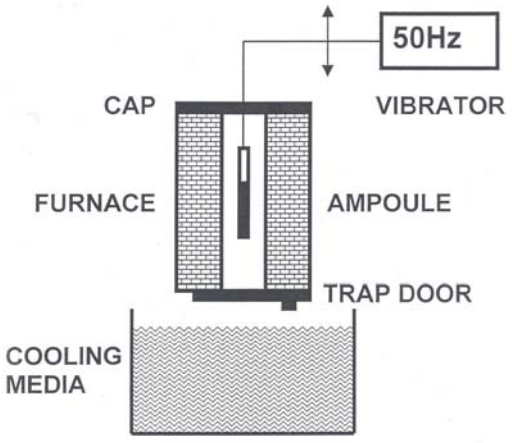

Fig. 2. Experimental set-up used for glass preparation.

Characterisation and quality of the samples were determined by X-ray diffraction (XRD) and differential scanning calorimetry (DSC). Infrared transmission windows were determined by optical absorption edge (E_g) measurements and far infrared transmission spectra (cut-off wavelength, λ_c).

For XRD experiments, powdered samples were ground manually and placed in a special support. Experiments were carried out on an automated Phillips diffractometer in the bragg-Brentano (θ-2θ) geometry. The patterns were run with Cu as target using the Kα filtered radiation (Ni filter, λ = 1.54 Å) at 40 keV and 20 mA, and scintillation registration, and were obtained in the range 5-30° in the θ scale within multiscan mode. Scanning rate was 0.04°θ/s, counting rate was 500 ms and we used 30 scans.

Glass transition temperature (Tg) measurements and thermal behavior were investigated by using a SETARAM DSC 121 differential scanning calorimeter. The temperature calibration were performed using the well known melting temperature of high-purity indium supplied with the instrument. The crystallization thermograms were recorded as the temperature of the samples increased at uniform rate using a dynamic argon atmosphere. Typically, 50mg of sample in powdered form (particle size less than 20µm) were sealed in standard quartz tube and scanned over a temperature range from room temperature to about 873K at heating rate α = 10K/min. The values of the glass transition temperature (Tg), the crystallization peaks (Tc_1, Tc_2) and the melting temperature (T_m) were determined with accuracy ±4K by using the microprocessor of the thermal analyser. Values are reported in Table 1. The densities were measured using the Archimedean method along with toluene as a reference medium.

Table 1. The ratio [Te]/([Te]+[As]) is taken in order to compare $Ge_{10}As_{90-x}Te_x$ and $Ge_{20}Te_{80}$ glasses. This ratio increases when Te content x increases. Densities are given in $g.cm^{-3}$. Optical absorption edges (E_g) are given in eV. Glass transition temperature (T_g), first (Tc_1) and eventually second (Tc_2) crystallisation temperature, and melting temperature of glassy compositions are given in K (error bars ±4K).

Composition	[Te]/ ([Te]+[As])	Density (±0.18)	Eg (±0.03)	Tg	Tc_1	Tc_2	Tc_1-Tg	T_m
$Ge_{10}As_{54}Te_{36}$	0.400	5.26	-	461	580	-	119	639
$Ge_{10}As_{50}Te_{40}$	0.444	5.54	0.92	449	549	571	100	649
$Ge_{10}As_{46}Te_{44}$	0.488	5.34	0.89	439	539	550	100	651
$Ge_{10}As_{20}Te_{70}$	0.777	5.63	0.83	403	442	497	39	628
$Ge_{10}As_{16}Te_{74}$	0.822	5.32	0.81	397	433	506	36	648
$Ge_{10}As_{10}Te_{80}$	0.888	-	0.79	385	449	504	64	645
$Ge_{20}Te_{80}$	1.000	5.26	0.72	420	443	503	23	640

Infrared transmission windows were determined by coupling optical absorption edges measurements (Eg given in **Table 1**) at low wavelengths (UV-visible and near infrared) and infrared transmission at medium and high wavelengths. First, we used a Beckman Acta M IV 5240 equipped with an integration sphere (0.5-3.5eV). Second, the experimental device was a FT-IR BOMEM DA 8 (2.5-50 µm). Samples were ground, mixed with powdered KBr, the pressed into pallets 13mm diameter and 0.4mm thick. As a example, the transmission window for the $Ge_{10}As_{20}Te_{70}$ glassy sample is given in Fig. 3.

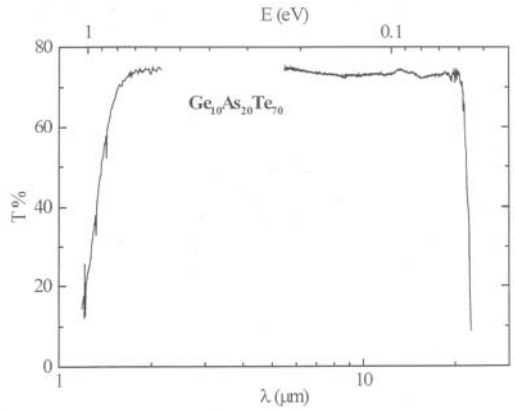

Fig. 3. Transmission window of $Ge_{10}As_{20}Te_{70}$ glassy sample. Low wavelengths spectrum was obtained from optical absorption edge measurements.

3. Results and discussion

3.1 Glass forming ability

Numerous trials were carried out in order to optimize the quenching process (ampoule size, cooling media, melt temperature, batch weight). It was performed for $Ge_{20}Te_{80}$ as can be seen in Fig. 4. Trials at 870°C and 900°C (melt temperature before quenching) clearly show XRD peaks of two crystalline phases c-GeTe and c-Te. At 960°C, broad bumps, typical for the glassy state, appear in the background. Some peaks still presents in the XRD pattern of the sample quenched at 1000°C in liquid nitrogen. For the same temperature, the melt quenched in iced water give a glassy sample without crystalline phases. This latter procedure was used for ternary compositions. The glassy nature of the synthesized materials has been confirmed by the absence of peaks in XRD patterns of annealed (50°C below T_g) samples as can be seen in Fig. 5. Broad bumps are typical for the glassy state. The position of observed bumps is slightly shifted towards small values of θ with the tellurium content.

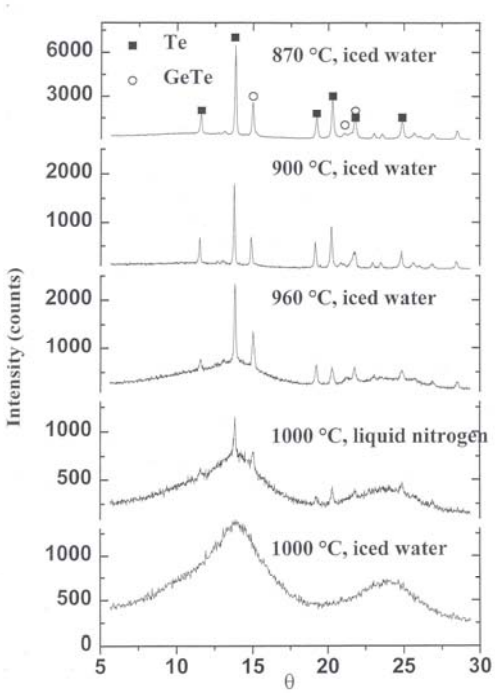

Fig. 4. X-Ray diffraction patterns of as-quenched samples as a function of the melting temperature and the cooling media for the $Ge_{20}Te_{80}$ composition. Observed diffraction peaks were attributed to the c-Te (■) and c-GeTe (o) crystalline phases.

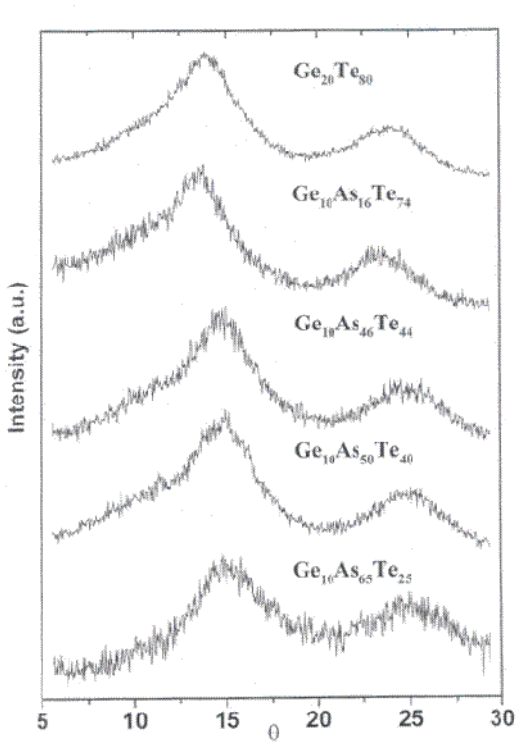

Fig. 5. X-ray diffraction patterns of glassy samples under investigation.

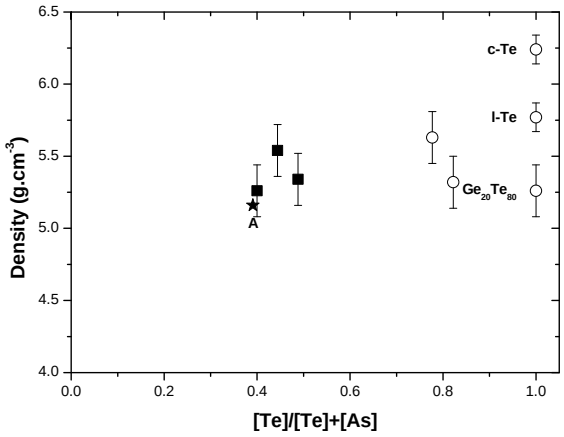

Fig. 6. Evolution of the density as a function of the ratio [Te]/([Te]+[As]). Glassy g-As_2Te_3 and g- $Ge_{20}Te_{80,}$ crystalline c- As_2Te_3 and c-Te and liquid Te at 725K are drawn for comparison. Open circles (o) correspond to 'Te-rich' glasses. Solid squares (■) correspond to 'As-rich' glasses. The star labeled A corresponds to $Sb_{12}As_{28}Se_{42}Te_{18}$ glassy composition.

Variations of the densities of $Ge_{10}As_{90-x}Te_x$ glassy samples as a function of the ratio [Te]/([Te]+ [As]) are represented in Figure 6.

3.2Thermal behavior and optical properties

T_g measured by DSC in plotted as function of the ratio [Te]/([Te]+ [As]) in Fig. 7. For the $Ge_{10}As_{90-x}Te_x$ samples, Tg continuously decreases from 461K (x = 36) to 385K (x = 80) with the Te content. After DSC measurements above melting temperature, samples present pronounced changes in the XRD patterns. It is clear that crystallization took place, resulting in the formation of phases which may be identified as Te, As, As_2Te_3, As_2GeTe_4 and $As_2Ge_3Te_6$ as can be seen in Fig. 8. Variation of the absorption edges (E_g), represented in Fig. 9**,** is very small due to similar electronic behavior for As and Te. On the contrary, glass transition temperature variations can be explained because of the substitution of As for Te in terms of connectivity.

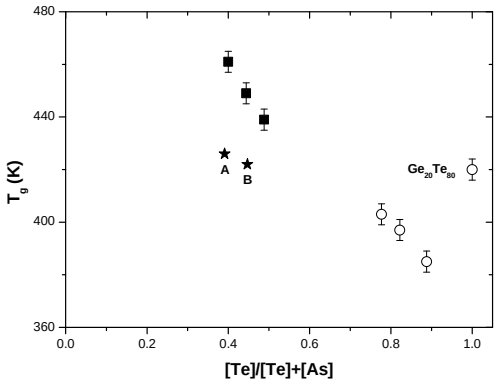

Fig. 7. Evolution of the glass transition temperature (T_g) as a function of the ratio [Te]/([Te]+[As]). Open circles (o) correspond to 'Te-rich' glasses. Solid squares (■) correspond to 'As-rich' glasses. Stars labeled A and B correspond to $Sb_{12}As_{28}Se_{42}Te_{18}$ and $Sb_{14}As_{26}Se_{39}Te_{21}$ glassy compositions respectively.

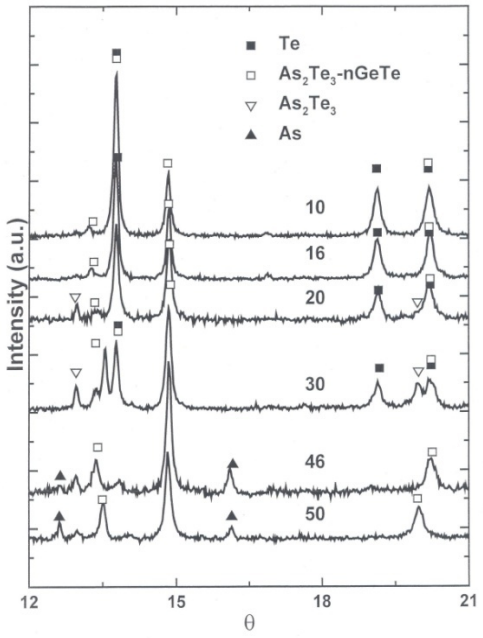

Fig. 8. X-ray diffraction patterns of annealed samples after DSC measurements. Different crystalline phases have been attributed: c-Te and $As_2Ge_3Te_6$ in the 'Te-rich' region, and As and As_2GeTe_4 in the 'As-rich' region.

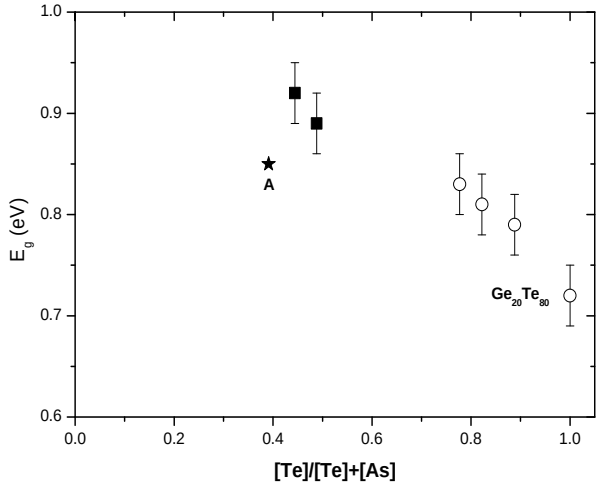

Fig. 9. Evolution of the optical absorption edge (E_g) as a function of the ratio [Te]/([Te]+[As]). Open circles (o) correspond to 'Te-rich' glasses. Solid squares (■) correspond to 'As-rich' glasses. The star labeled A corresponds to $Sb_{12}As_{28}Se_{42}Te_{18}$ glassy composition.

3.3 Relationship between T_g and connectivity

For each sample only one value of glass transition temperature (Tg) was measured by DSC. Decrease of Tg values with the Te content for $Ge_{10}As_{90-x}Te_x$ glasses can be explained by a decrease of the network rigidity. Usual co-ordination numbers (8-N rule) for the Te, As and Ge atoms in chalcogenide glasses are 2, 3 and 4 respectively. The compositional variation of the investigated glasses is characterized by the Te-concentration (x at. %) and/or by the average co-ordination number Z[21,22]. For the $Ge_{10}As_{90-x}Te_x$ glasses the average co-ordination number is $Z = 3.1-0.01x$.

A model commonly used is the Sreeram's model [23,24] based on Gibbs and Di Marzio's work. In this model the authors assume that glasses are formed by chains of twofold co-ordinated atoms (S, Se, or Te in chalcogenide glasses). They make the assumption that T_0 equals to T_g for the ideal chalcogenide glasses (pure element) where Z equals 2.

Considering thus the average co-ordination number Z, Tg is rules by the following law: $T_g = T_0/[1-\beta(Z-2)]$ where β is characteristic of the system. Hence drawing $1000/T_g$ as a function of the cross-linking density (Z-2) gives an estimated value for $1000/T_0$. Values obtained in this work are $T_0 = 340\pm4$K and $1/\beta = 0.40\pm0.02$ for the $Ge_{10}As_{90-x}Te_x$ glasses. As a comparison we give here results obtained for binary $T_0 = 343$K in tellurium, $T_0 = 316$ K in selenium, $T_0 = 245$ K in sulfur based glasses [25,26].

3.4 Relationship between T_g and E_g

Values reported in **tables 1** and **2** have been used to show (see Fig. 10) the correlation between T_g , which reflects the covalency of the chemical bonding between glassy micro domains, and E_g, which is the rigidity of the molecular units composing the micro domains. The linear correlation for the both groups ('Te-rich' and 'As-rich' glasses) dearly show that molecular units are the same and have similar structural behavior. These results are in a good agreement with those previously reported [16, 17].

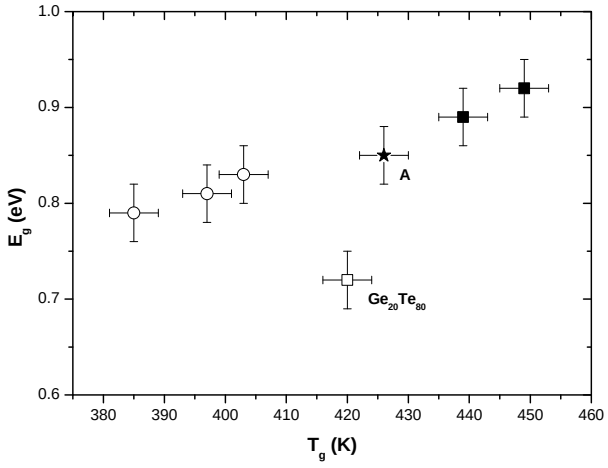

Fig. 10. Correlation between optical gap (E_g) and glass transition temperatures (T_g) for compositions described in this study. Open circles (o) correspond to 'Te-rich' glasses. Solid squares (■) correspond to 'As-rich' glasses. The star labeled A corresponds to $Sb_{12}As_{28}Se_{42}Te_{18}$ glassy composition.

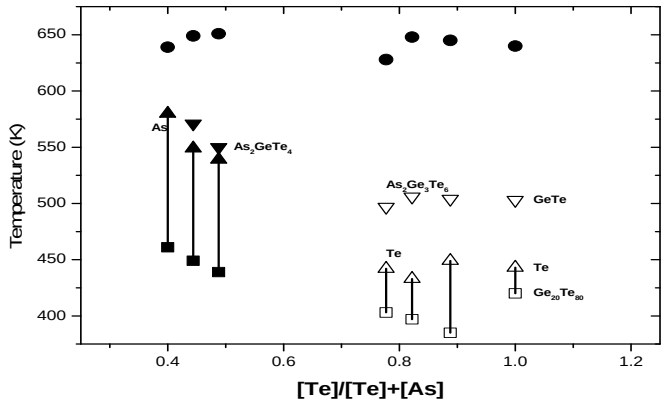

Fig. 11. Representation of the thermal behaviour of the glassy samples. Glass transition temperatures (■□), crystallisation temperature (▲▼Δ∇) and melting point (●) are draw as a function of the ratio [Te]/ ([Te]+[As]). Solid lines are drawn in order to give an idea of the thermal stability of the glassy compositions and represent (Tc_1-Tg) quantity. (see text for details)

3.5 Comparison with the values obtained in the binary system Sb_2Te_3-As_2Se_3

The values of the ratio [Te]/([Te]+[As]) of the compositions $Ge_{10}As_{54}Te_{36}$ (0.400) and $Ge_{10}As_{50}Te_{40}$ (0.444) of the system Ge-As-Te itself close to those of the compositions $Sb_{12}As_{28}Se_{42}Te_{18}$ (0.391) and $Sb_{14}As_{26}Se_{39}Te_{21}$ (0.447) of the Sb_2Te_3-As_2Se_3 system we can thus compare their physical properties (ρ, Eg, Tg, Tc_1, Tc_2, Tc_1-Tg and T_m) (**Table 2**).

Table 2. Comparison of the values of the physical properties (ρ, Eg, Tg, Tc_1, Tc_2, Tc_1-Tg and T_m) of two compositions of the ternary system Ge-As-Te those their counterparts of the Sb_2Te_3-As_2Se_3 binary system.

Compositions	[Te]/ ([Te]+ [As])	Density (±0.18)	Eg (±0.03)	Tg	Tc_1	Tc_2	Tc_1-Tg	T_m
$Ge_{10}As_{54}Te_{36}$	0.400	5.26	-	461	580	-	119	639
$Sb_{12}As_{28}Se_{42}Te_{18}$ (A)	0.391	5.16	0.85	426	478	525	52	607
$Ge_{10}As_{50}Te_{40}$	0.444	5.54	0.92	449	549	571	100	649
$Sb_{14}As_{26}Se_{39}Te_{21}$ (B)	0.447	---	---	422	456	517	34	580

When one replaces germanium by selenium and antimony in the ternary system Ge-As-Te, one notes that the values of the physical properties evolve in the same direction when the ratio [Te]/([Te] + [As]) increases, but they hhave lower values in the system Sb_2Te_3-As_2Se_3. The aptitude to vitrify glasses of this system (Ge-As-Te) is more important, proving that these are more stable than those of the system Sb_2Te_3-As_2Se_3.

3.6 Crystallization process

In Fig. 11, we have represented the thermal behavior (characteristic temperatures) as a function of the ratio [Te]/([Te]+ [As]). We proposed from XRD patterns and DSC measurements the following crystallization process. In the 'Te-rich' region, crystallization occurs at ~440K for c-Te and at ~500K for $As_2Ge_3Te_6$. The crystallization process follows the reaction::

$$g\text{-}\ Ge_{10}As_{90-x}Te_x (70 \leq x \leq 80 \rightarrow c\text{-}Te + c\text{-}\ As_2Ge_3Te_6$$

In the 'As-rich' region, it occurs above 540K for c-As and As_2GeTe_4 and depends on the composition. In this case, the crystallization process is:

$$g\text{-}\ Ge_{10}As_{90-x}Te_x (40 \leq x \leq 60 \rightarrow c\text{-}As + c\text{-}As_2GeTe_4$$

For all compositions, melting point occurs in the range [630-650K].

Concerning the thermal stability of the compositions under study, we can see in Fig. 11 the 'As-rich' glasses present a more stable thermal domain than 'Te-rich' glasses. Hence, these compositions are more suitable for drawing glassy fibers devoted to IR sensors technology.

4. Conclusions

We investigated some ternary compositions in the Ge-As-Te system. Particular attention was made in the preparation of the glassy sample. We have optimized the quenching process in order to produce glasses avoiding crystallization. Then, optical properties of these glasses have been studied. Fundamental study of relationships between structure and properties are very important to decide if telluride glasses constitute good candidates for devices involving good optical transmission in the far infrared domain. We also studied their thermal stability in order to choose a glass presenting optimal performance for drawing fibers without crystalline domains. A comparison of the properties of glasses of the ternary system Ge-As-Te was done with those of glasses of the binary system Sb_2Te_3-As_2Se_3. It made it possible to show that the substitution of germanium by selenium and antimony reduces the physical properties (ρ, Eg, Tg, Tc_1, Tc_2, Tc_1-Tg et T_m). Indeed germanium supports the formation of glasses, contrary to metal antimony.

References

[1] C.H. Seager, D. Emin, R.K. Quinn, Phys. Rev., **B8,** 4746 (1973).

[2] H. Krebs, P. Fischer, Discuss. Farad., **50,** 35 (1970).
[4] A.B. Seddon, J. Non Cryst. Solids, **184,** 44 (1995).
[5] S.S.K. Titus, S. Asokan, T.S. Panchapagesan, E.S.R. Gopal, Phys. Rev., **B46,** 14493 (1992).
[6] S. Asokan, E.S.R. Gopal, Rev. Solid State Sci., **3,** 273 (1989).
[7] J.A. Savage, S. Nielsen, Phys. Chem. Glasses, **7**, 56 (1966).
[8] P.P. Seregin, V.P. Sivkov, F.S. Nasredinov, L.N. Vasilev, Yu V. Krylnikov, Yu P. Kostinov, Phys. Stat. Sol. (a) **39,** 437 (1977).
[9] B. Bureau, S. Danto, H. Li Ma, C. Boussard-Plédel, X. H. Zhang, J. Lucas, Solid State Sciences **10**, 427 (2008).
[10] J. Cornet, D. Rossier, J. Non Cryst. Solids, **12,** 61 (1973).
[11] D.J. Sarach, J.P. de Neufville, W.L. Haworth, J. Non Cryst. Solids, **22,** 245 (1976).
[12] H.W. Shu, S. Jaulmes, J. Flahaut, J. Solid State Chem., **74,** 277 (1988).
[13] R. Ollitrault-Fichet, H.W. Shu, J.Rivet, J. Flahaut, Mat. Res. Bull. **24,** 351 (1989).
[14] A.R. Hilton, C.E. Jones, M. Brau, Infrared Phys. **6,** 183 (1966).
[15] J.A. Savage, J. Non Cryst. Solids, **11,** 121 (1972).
[16] J.A. Savage, J. Mater. Sci., **6,** 964 (1971).
[17] P.E. Lippens, J.C. Jumas, J. Olivier-Fourcade, L. Aldon, J. Non Cryst. Solids, **271,** 119 (2000).
[18] L. Aldon, P.E. Lippens, J.C. Jumas, J. Olivier-Fourcade, H. Bemelmans, G. Langouche, J. Non Cryst. Solids, **262,** 244 (2000).
[19] P.E. Lippens, J.C. Jumas, J. Olivier-Fourcade, L. Aldon, J. Phys. Chem. Solids, **61,** 1761 (2000).
[20] L. Aldon, Ph. D thesis (December 1996), Université Montpellier II, France.
[21] K. Tanaka, Phys. Rev., **B39,** 1270 (1989).
[22] J.P. de Neufville, H.K. Rockstad, Proc. Amorphous Solids and Liquid semiconductors, 449 (1974).
[23] A.N. Sreeram, D.R. Swiler, A.J.K. Varshneya, J. Non Cryst. Solids, **127,** 287 (1991).
[24] A.J.K. Varshneya, A.N. Sreeram, D.R. Swiler, Phys. Chem. Glasses, **34,** 179 (1993).
[25] R. Kerner, M. Micoulaut, J. Non Cryst. Solids, **210,** 298 (1997).
[26] M. Micoulaut, Eur. Phys. J., **B1,** 277 (1998).